Charmless $B \to K_h \eta^{(\prime)}$ decays with $K_h = K, K^*, K_0^*(1430), K_2^*(1430)$

Hai-Yang Cheng[1,2] and Chun-Khiang Chua[3]

[1]*Institute of Physics, Academia Sinica, Taipei, Taiwan 115, Republic of China*
[2]*Physics Department, Brookhaven National Laboratory, Upton, New York 11973*
[3]*Department of Physics, Chung Yuan Christian University, Chung-Li, Taiwan 320, Republic of China*
(Received 13 May 2010; published 12 August 2010)

We study the charmless decays $B \to K_h \eta$ and $B \to K_h \eta'$ within the framework of QCD factorization (QCDF) for $K_h = K, K^*, K_0^*(1430)$ and naive factorization for $K_h = K_2^*(1430)$. There are three distinct types of penguin contributions: (i) $b \to sq\bar{q} \to s\eta_q$, (ii) $b \to ss\bar{s} \to s\eta_s$, and (iii) $b \to sq\bar{q} \to q\bar{K}_h$, where $\eta_q = (u\bar{u} + d\bar{d})/\sqrt{2}$ and $\eta_s = s\bar{s}$. $B \to K^{(*)}\eta^{(\prime)}$ decays are dominated by type-II and type-III penguin contributions. The interference, constructive for $K\eta'$ and $K^*\eta$ and destructive for $K\eta$ and $K^*\eta'$, between type-II and type-III diagrams explains the pattern of $\Gamma(B \to K\eta') \gg \Gamma(B \to K\eta)$ and $\Gamma(B \to K^*\eta') \ll \Gamma(B \to K^*\eta)$. Within QCDF, the observed large rate of the $K\eta'$ mode can be naturally explained without invoking flavor-singlet contributions or something exotic. The decay pattern for $B \to K_0^*(1430)\eta^{(\prime)}$ decays depends on whether the scalar meson $K_0^*(1430)$ is an excited state of κ or a lowest-lying P-wave $q\bar{q}$ state. Hence, the experimental measurements of $B \to K_0^*(1430)\eta^{(\prime)}$ can be used to explore the quark structure of $K_0^*(1430)$. If $K_0^*(1430)$ is a low-lying $q\bar{q}$ bound state, we find that $K_0^*\eta$ has a rate slightly larger than $K_0^*\eta'$ owing to the fact that the $\eta - \eta'$ mixing angle in the η_q, η_s flavor basis is less than $45°$, in agreement with experiment. The type-III penguin diagram does not contribute to $B \to K_2^*\eta^{(\prime)}$ under the factorization hypothesis and the type-II diagram dominates. The ratio $\Gamma(B \to K_2^*\eta')/\Gamma(B \to K_2^*\eta)$ is expected to be of order 2.5 as a consequence of (i) $|f_{\eta'}^s| > |f_\eta^s|$ and (ii) a destructive (constructive) interference between type-I and type-II penguin diagrams for $K_2^*\eta$ ($K_2^*\eta'$). However, the predicted rates of $B \to K_2^*\eta^{(\prime)}$ in naive factorization are too small by 1 order of magnitude and this issue remains to be resolved. There are two $K^{(*)}\eta^{(\prime)}$ modes in which direct CP asymmetries have been measured with significance around 4σ: $A_{CP}(K^-\eta) = -0.37 \pm 0.09$ and $A_{CP}(\bar{K}^{*0}\eta) = 0.19 \pm 0.05$. In QCDF, power corrections from penguin annihilation which are needed to resolve CP puzzles in $K^-\pi^+$ and $\pi^+\pi^-$ modes will flip $A_{CP}(K^-\eta)$ into a wrong sign. We show that soft corrections to the color-suppressed tree amplitude a_2 in conjunction with the charm content of the η will finally lead to $A_{CP}(K^-\eta) = -0.15^{+0.19}_{-0.28}$. Likewise, this power correction is needed to improve the prediction for $A_{CP}(\bar{K}^{*0}\eta)$.

I. INTRODUCTION

Recently *BABAR* has measured charmless B decays with final states containing η or η' [1]. Comparing the first measurements of $B \to K_0^*(1430)\eta'$ and $B \to K_2^*(1430)\eta'$ by *BABAR* with previous results of $B \to K_0^*(1430)\eta$ and $B \to K_2^*(1430)\eta$ (see Table I) clearly indicates that $\mathcal{B}(B \to K_0^*(1430)\eta') < \mathcal{B}(B \to K_0^*(1430)\eta)$ and $\mathcal{B}(B \to K_2^*(1430)\eta') > \mathcal{B}(B \to K_2^*(1430)\eta)$. It is well known that $\mathcal{B}(B \to K\eta') \gg \mathcal{B}(B \to K\eta)$ and $\mathcal{B}(B \to K^*\eta') \ll \mathcal{B}(B \to K^*\eta)$. The last two patterns can be understood as the interference between the dominant penguin amplitudes.

For the η and η' particles, it is more convenient to consider the flavor states $q\bar{q} \equiv (u\bar{u} + d\bar{d})/\sqrt{2}$, $s\bar{s}$, and $c\bar{c}$ labeled by the η_q, η_s, and η_c^0, respectively. Neglecting the small mixing with η_c^0, we write

$$\begin{pmatrix} |\eta\rangle \\ |\eta'\rangle \end{pmatrix} = \begin{pmatrix} \cos\phi & -\sin\phi \\ \sin\phi & \cos\phi \end{pmatrix} \begin{pmatrix} |\eta_q\rangle \\ |\eta_s\rangle \end{pmatrix}, \qquad (1)$$

where $\phi = (39.3 \pm 1.0)°$ [3] is the $\eta - \eta'$ mixing angle in the η_q and η_s flavor basis. Three different penguin con-

tributions are depicted in Fig. 1: (i) $b \to sq\bar{q} \to s\eta_q$, (ii) $b \to ss\bar{s} \to s\eta_s$, and (iii) $b \to sq\bar{q} \to q\bar{K}_h$, corresponding to Figs. 1(a)–1(c), respectively. For $B \to K^{(*)}\eta^{(\prime)}$ decays, the dominant penguin amplitudes arise from Figs. 1(b) and 1(c) governed by the parameters $\alpha_4(K_h\eta_s)$ and $\alpha_4(\eta_q K_h)$, respectively. Their expressions in terms of the effective Wilson coefficients a_4 and a_6 are summarized in Table II.

It is clear that the interference between the $B \to K\eta_q$ amplitude induced by the $b \to sq\bar{q}$ penguin and the $B \to K\eta_s$ amplitude induced by $b \to ss\bar{s}$ is constructive for $B \to K\eta'$ and destructive for $B \to K\eta$. This explains the large rate of the former and the suppression of the latter [4]. For $B \to K^*\eta^{(\prime)}$ decays, it is the other way around. The sign difference between $\alpha_4(\eta_q K^*)$ and $\alpha_4(K^*\eta_s)$ explains why $\Gamma(B \to K^*\eta) \gg \Gamma(B \to K^*\eta')$, recalling that a_4 and a_6 are negative and the magnitude of the latter is larger than the former and that the chiral factor r_χ to be defined below is of order unity for light mesons.

The decay pattern for $B \to K_0^*(1430)\eta^{(\prime)}$ decays depends on whether $K_0^*(1430)$ is an excited state of κ [or $K_0^*(800)$]

TABLE I. Experimental branching fractions (in units of 10^{-6}) of $B \to K_h \eta^{(')}$ with $K_h = K$, K^*, $K_0^*(1430)$, and $K_2^*(1430)$ taken from [1,2].

	$K\eta$	$K\eta'$	$K^*\eta$	$K^*\eta'$	$K_0^*\eta$	$K_0^*\eta'$	$K_2^*\eta$	$K_2^*\eta'$
B^+	2.36 ± 0.27	71.1 ± 2.6	19.3 ± 1.6	$4.9^{+2.1}_{-1.9}$	15.8 ± 3.1	5.2 ± 2.1	9.1 ± 3.0	$28.0^{+5.3}_{-5.0}$
B^0	$1.12^{+0.30}_{-0.28}$	66.1 ± 3.1	15.9 ± 1.0	3.8 ± 1.2	9.6 ± 1.9	6.3 ± 1.6	9.6 ± 2.1	$13.7^{+3.2}_{-3.1}$
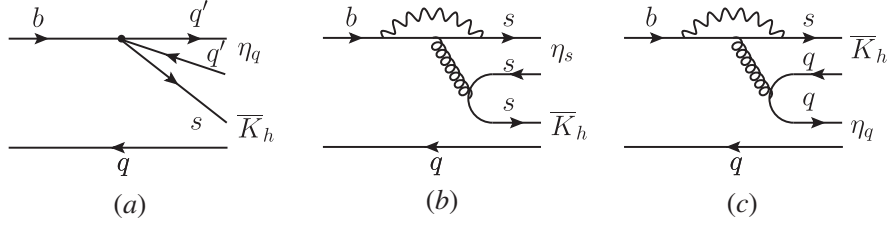
FIG. 1. Three different penguin contributions to $\bar{B} \to \bar{K}_h \eta^{(')}$ with K_h denoting K, K^*, $K_0^*(1430)$, and $K_2^*(1430)$. Figure 1(a) is induced by the penguin operators $O_{3,5,7,9}$.

or a low-lying P-wave $q\bar{q}$ state. Hence, the experimental measurements of $B \to K_0^*(1430)\eta^{(')}$ can be used to explore the quark structure of the scalar meson $K_0^*(1430)$. A detailed study in this work shows that $\Gamma(B \to K_0^*\eta) \ll \Gamma(B \to K_0^*\eta')$ in the first scenario for $K_0^*(1430)$ and $\Gamma(B \to K_0^*\eta) > \Gamma(B \to K_0^*\eta')$ in the latter scenario. As for $B \to K_2^*(1430)\eta^{(')}$ decays, Fig. 1(c) does not make contribution owing to the vanishing decay constant of K_2^*. Since the interference between Figs. 1(a) and 1(b) is constructive for $K_2^*\eta'$ and destructive for $K_2^*\eta$ and since the decay constant $f_{\eta'}^s$ is larger than f_η^s, one will expect a larger rate for $K_2^*\eta'$ than $K_2^*\eta$.

Recently we have studied the decays $B \to (K, K^*)\eta^{(')}$ within the framework of QCD factorization (QCDF) [5,6]. Here we shall present updated results with some discussions. Then in the rest of this work we will focus on $B \to (K_0^*(1430), K_2^*(1430))\eta^{(')}$ decays and study their decay pattern.

The layout of the present paper is as follows. In Sec. II we recapitulate the framework of QCD factorization. Then we proceed to study $B \to (K, K^*)(\eta, \eta')$ decays in Sec. III and $B \to K_0^*(1430)(\eta, \eta')$ decays in Sec. IV. Because the QCDF approach for the $K_2^*(1430)\eta^{(')}$ modes has not been developed, we rely on naive factorization to study the tensor meson production in Sec. V. Section VI presents

our conclusions. An appendix is devoted to the decay constants and matrix elements of the η and η' mesons.

II. QCD FACTORIZATION

Within the framework of QCDF [7], the effective Hamiltonian matrix elements are written in the form

$$\langle M_1 M_2 | \mathcal{H}_{\text{eff}} | \bar{B} \rangle = \frac{G_F}{\sqrt{2}} \sum_{p=u,c} \lambda_p^{(q)} \langle M_1 M_2 | \mathcal{T}_\mathcal{A}^p + \mathcal{T}_\mathcal{B}^p | \bar{B} \rangle,$$

(2)

where $\lambda_p^{(q)} = V_{pb} V_{pq}^*$ with $q = s, d$, $\mathcal{T}_\mathcal{A}$ describes contributions from naive factorization, vertex corrections, penguin contractions, and spectator scattering expressed in terms of the flavor operators a_i^p, while $\mathcal{T}_\mathcal{B}$ contains annihilation topology amplitudes characterized by the annihilation operators b_i^p. The explicit expressions of $\mathcal{T}_\mathcal{A}$ and $\mathcal{T}_\mathcal{B}$ can be found in [7,8]. In practice, it is more convenient to express the decay amplitudes in terms of the flavor operators α_i^p and the annihilation operators β_i^p. Their relations to the coefficients a_i^p and b_i^p will be specified below.

The expressions of $\bar{B} \to \bar{K}_h \eta^{(')}$ decay amplitudes for $K_h = K$, K^*, $K_0^*(1430)$, and $K_2^*(1430)$ are given by [8]

TABLE II. The parameters $\alpha_4(K_h\eta_s)$ and $\alpha_4(\eta_q K_h)$ with $K_h = K$, K^*, $K_0^*(1430)$, and $K_2^*(1430)$.

	K	K^*	$K_0^*(1430)$	$K_2^*(1430)$
$\alpha_4(K_h\eta_s)$	$a_4 + r_\chi^{\eta_s} a_6$	$a_4 - r_\chi^{\eta_s} a_6$	$a_4 - r_\chi^{\eta_s} a_6$	$a_4 - r_\chi^{\eta_s} a_6$
$\alpha_4(\eta_q K_h)$	$a_4 + r_\chi^K a_6$	$a_4 + r_\chi^{K^*} a_6$	$a_4 - r_\chi^{K_0^*} a_6$	-

$$\sqrt{2} A_{B^- \to K_h^- \eta^{(\prime)}} = X^{(\bar{B} \bar{K}_h, \eta_q^{(\prime)})} [\delta_{pu}(\alpha_2 + 2\beta_{S2}) + 2\alpha_3^p + \frac{1}{2}\alpha_{3,\mathrm{EW}}^p + 2\beta_{S3}^p + 2\beta_{S3,\mathrm{EW}}^p] + \sqrt{2} X^{(\bar{B} \bar{K}_h, \eta_s^{(\prime)})} [\delta_{pu}(\beta_2 + 2\beta_{S2}) + \alpha_3^p$$

$$+ \alpha_4^p - \frac{1}{2}\alpha_{3,\mathrm{EW}}^p - \frac{1}{2}\alpha_{4,\mathrm{EW}}^p + \beta_3^p + \beta_{3,\mathrm{EW}}^p + \beta_{S3}^p + \beta_{S3,\mathrm{EW}}^p] + \sqrt{2} X^{(\bar{B} \bar{K}_h, \eta_c^{(\prime)})} [\delta_{pc}\alpha_2 + \alpha_3^p]$$

$$+ X^{(\bar{B} \eta_q^{(\prime)}, \bar{K}_h)} [\delta_{pu}(\alpha_1 + \beta_2) + \alpha_4^p + \alpha_{4,\mathrm{EW}}^p + \beta_3^p + \beta_{3,\mathrm{EW}}^p],$$

$$\sqrt{2} A_{\bar{B}^0 \to \bar{K}_h^0 \eta^{(\prime)}} = X^{(\bar{B} \bar{K}_h, \eta_q^{(\prime)})} \left[\delta_{pu}\alpha_2 + 2\alpha_3^p + \frac{1}{2}\alpha_{3,\mathrm{EW}}^p + 2\beta_{S3}^p - \beta_{S3,\mathrm{EW}}^p \right] + \sqrt{2} X^{(\bar{B} \bar{K}_h, \eta_s^{(\prime)})} \left[\alpha_3^p + \alpha_4^p - \frac{1}{2}\alpha_{3,\mathrm{EW}}^p - \frac{1}{2}\alpha_{4,\mathrm{EW}}^p \right.$$

$$+ \beta_3^p - \frac{1}{2}\beta_{3,\mathrm{EW}}^p + \beta_{S3}^p - \frac{1}{2}\beta_{S3,\mathrm{EW}}^p \right] + \sqrt{2} X^{(\bar{B} \bar{K}_h, \eta_c^{(\prime)})} [\delta_{pc}\alpha_2 + \alpha_3^p]$$

$$+ X^{(\bar{B} \eta_q^{(\prime)}, \bar{K}_h)} \left[\alpha_4^p - \frac{1}{2}\alpha_{4,\mathrm{EW}}^p + \beta_3^p - \frac{1}{2}\beta_{3,\mathrm{EW}}^p \right]. \tag{3}$$

The order of the arguments of $\alpha_i^p(M_1 M_2)$ and $\beta_i^p(M_1 M_2)$, which are not shown explicitly here, is consistent with the order of the arguments of the factorizable matrix elements $X^{(\bar{B} M_1, M_2)}$ given by

$$X^{(\bar{B} P_1, P_2)} \equiv \langle P_2 | J^\mu | 0 \rangle \langle P_1 | J'_\mu | \bar{B} \rangle = i f_{P_2}(m_B^2 - m_{P_1}^2) F_0^{B P_1}(m_{P_2}^2), \qquad X^{(\bar{B} P, V)} \equiv \langle V | J^\mu | 0 \rangle \langle P | J'_\mu | \bar{B} \rangle = 2 f_V m_B p_c F_1^{BP}(m_V^2),$$

$$X^{(\bar{B} V, P)} \equiv \langle P | J^\mu | 0 \rangle \langle V | J'_\mu | \bar{B} \rangle = 2 f_P m_B p_c A_0^{BV}(m_P^2), \qquad X^{(\bar{B} P, S)} \equiv \langle S | J^\mu | 0 \rangle \langle P | J'_\mu | \bar{B} \rangle = f_S(m_B^2 - m_P^2) F_0^{BP}(m_S^2),$$

$$X^{(\bar{B} S, P)} \equiv \langle P | J^\mu | 0 \rangle \langle S | J'_\mu | \bar{B} \rangle = -f_P(m_B^2 - m_S^2) F_0^{BS}(m_P^2),$$

$$X^{(\bar{B} T, P)} \equiv \langle P | J^\mu | 0 \rangle \langle T | J'_\mu | \bar{B} \rangle = -i f_P [k(m_P^2) + (m_B^2 - m_T^2) b_+(m_P^2) + m_P^2 b_-(m_P^2)] \varepsilon_{\mu\nu}^* p_B^\mu p_B^\nu,$$

$$X^{(\bar{B} P, T)} \equiv \langle T | J^\mu | 0 \rangle \langle P | J'_\mu | \bar{B} \rangle = 0, \tag{4}$$

where f_P, f_V, f_S are the decay constants of pseudoscalar, vector, and scalar mesons, respectively, and k, b_+, b_- are B to tensor meson transition form factors defined in Eq. (27) below.

The flavor operators α_i^p and the annihilation operators β_i^p are related to the coefficients a_i^p and b_i^p by

$$\alpha_1(M_1 M_2) = a_1(M_1 M_2), \qquad \alpha_2(M_1 M_2) = a_2(M_1 M_2),$$

$$\alpha_3^p(M_1 M_2) = \begin{cases} a_3^p(M_1 M_2) - a_5^p(M_1 M_2) & \text{for } M_1 M_2 = PP, VP, SP, TP \\ a_3^p(M_1 M_2) + a_5^p(M_1 M_2) & \text{for } M_1 M_2 = PV, PS, \end{cases}$$

$$\alpha_4^p(M_1 M_2) = \begin{cases} a_4^p(M_1 M_2) + r_\chi^{M_2} a_6^p(M_1 M_2) & \text{for } M_1 M_2 = PP, PV, \\ a_4^p(M_1 M_2) - r_\chi^{M_2} a_6^p(M_1 M_2) & \text{for } M_1 M_2 = VP, SP, PS, TP \end{cases} \tag{5}$$

$$\alpha_{3,\mathrm{EW}}^p(M_1 M_2) = \begin{cases} a_9^p(M_1 M_2) - a_7^p(M_1 M_2) & \text{for } M_1 M_2 = PP, VP, SP, TP \\ a_9^p(M_1 M_2) + a_7^p(M_1 M_2) & \text{for } M_1 M_2 = PV, PS, \end{cases}$$

$$\alpha_{4,\mathrm{EW}}^p(M_1 M_2) = \begin{cases} a_{10}^p(M_1 M_2) + r_\chi^{M_2} a_8^p(M_1 M_2) & \text{for } M_1 M_2 = PP, PV \\ a_{10}^p(M_1 M_2) - r_\chi^{M_2} a_8^p(M_1 M_2) & \text{for } M_1 M_2 = VP, SP, PS, TP, \end{cases}$$

and

$$\beta_i^p(M_1 M_2) = \frac{i f_B f_{M_1} f_{M_2}}{X^{(\bar{B} M_1, M_2)}} b_i^p, \tag{6}$$

where the chiral factors r_χ's are given by

$$r_\chi^P(\mu) = \frac{2m_P^2}{m_b(\mu)(m_2 + m_1)(\mu)},$$

$$r_\chi^{\eta_s} = \frac{h_P^s}{f_P^s m_b(\mu) m_s(\mu)},$$

$$r_\chi^V(\mu) = \frac{2m_V}{m_b(\mu)} \frac{f_V^\perp(\mu)}{f_V},$$

$$r_\chi^{K_0^*}(\mu) = \frac{2m_{K_0^*}^2}{m_b(\mu)(m_s - m_q)(\mu)}, \tag{7}$$

with the parameters f_P^s and h_P^s being defined in the Appendix.

The flavor operators a_i^p are basically the Wilson coefficients in conjunction with short-distance nonfactorizable corrections such as vertex corrections and hard spectator interactions. In general, they have the expressions [7,8]

$$a_i^p(M_1 M_2) = \left(c_i + \frac{c_{i \pm 1}}{N_c} \right) N_i(M_2) + \frac{c_{i \pm 1}}{N_c} \frac{C_F \alpha_s}{4\pi} \left[V_i(M_2) \right.$$

$$\left. + \frac{4\pi^2}{N_c} H_i(M_1 M_2) \right] + P_i^p(M_2), \tag{8}$$

where $i = 1, \ldots, 10$, the upper (lower) signs apply when i is odd (even), c_i are the Wilson coefficients, $C_F = (N_c^2 - 1)/(2N_c)$ with $N_c = 3$, M_2 is the emitted meson and M_1

shares the same spectator quark with the B meson. The quantities $V_i(M_2)$ account for vertex corrections, $H_i(M_1M_2)$ for hard spectator interactions with a hard gluon exchange between the emitted meson and the spectator quark of the B meson and $P_i(M_2)$ for penguin contractions. The expression of the quantities $N_i(M_2)$ reads

$$N_i(M_2) = \begin{cases} 0, & i = 6, 8 \quad \text{and} \quad M_2 = V \\ 1 & \text{else.} \end{cases} \qquad (9)$$

In Eq. (3), possible flavor-singlet penguin annihilation contributions are denoted by β_S's which will not be considered in this work.

Power corrections in QCDF always involve troublesome end-point divergences. For example, the annihilation amplitude has end-point divergences even at twist-2 level and the hard spectator scattering diagram at twist-3 order is power suppressed and possesses soft and collinear divergences arising from the soft spectator quark. Since the treatment of end-point divergences is model dependent, subleading power corrections generally can be studied only in a phenomenological way. We shall follow [7] to model the end-point divergence $X \equiv \int_0^1 dx/(1 - x)$ in the annihilation and hard spectator scattering diagrams as

$$\begin{aligned} X_A &= \ln\left(\frac{m_B}{\Lambda_h}\right)(1 + \rho_A e^{i\phi_A}), \\ X_H &= \ln\left(\frac{m_B}{\Lambda_h}\right)(1 + \rho_H e^{i\phi_H}), \end{aligned} \qquad (10)$$

with Λ_h being a typical scale of order 500 MeV, and $\rho_{A,H}$, $\phi_{A,H}$ being the unknown real parameters.

As pointed out in [6], while the discrepancies between experiment and theory in the heavy quark limit for the rates of penguin-dominated two-body decays of B mesons and direct CP asymmetries of $\bar{B}^0 \to K^- \pi^+$, $B^- \to K^- \rho^0$, and $\bar{B}^0 \to \pi^+ \pi^-$ are resolved by introducing power corrections coming from penguin annihilation, the signs of direct CP-violating effects in $B^- \to K^- \pi^0$, $B^- \to K^- \eta$, and $\bar{B}^0 \to \pi^0 \pi^0$ are flipped to the wrong ones when confronted with experiment. These new B-CP puzzles in QCDF can be resolved by the subleading power corrections to the color-suppressed tree amplitudes due to spectator interactions and/or final-state interactions [9] that not only reproduce correct signs for the aforementioned CP asymmetries but also accommodate the observed $\bar{B}_d \to \pi^0 \pi^0$ and $\rho^0 \pi^0$ rates simultaneously. Following [6], power corrections to the color-suppressed topology are parametrized as

$$a_2 \to a_2(1 + \rho_C e^{i\phi_C}), \qquad (11)$$

with the unknown parameters ρ_C and ϕ_C to be inferred from experiment.

For S-wave mesons, input parameters such as decay constants, form factors, quark masses, Wolfenstein parameters, light-cone distribution amplitudes, and power correction parameters can be found in [5]. Input parameters for parity-even mesons such as $K_0^*(1430)$ and $K_2^*(1430)$

will be specified later. For the renormalization scale of the decay amplitude, we choose $\mu = m_b(m_b) = 4.2$ GeV.

III. $B \to (K, K^*)(\eta, \eta')$ DECAYS

A. Branching fractions

Details of the calculations in the framework of QCDF for all $B \to PP$, VP decays can be found in [5,6]. The updated results for the branching fractions and direct CP asymmetries in $B \to K^{(*)}\eta^{(')}$ decays are exhibited in Table III after correcting some minor errors in the previous computer codes.

Numerically, Beneke and Neubert already obtained $\mathcal{B}(B^- \to K^- \eta') \sim \mathcal{O}(50 \times 10^{-6})$ in QCDF using the default values $\rho_A = \rho_H = 0$ [8]. Here we found similar results 57×10^{-6} (53×10^{-6}) with (without) the contributions from the "charm content" of the η'. In the presence of penguin annihilation, we obtain $\mathcal{B}(B^- \to K^- \eta') \sim 75 \times 10^{-6}$ (67×10^{-6}) with (without) the charm content contributions. Therefore, the observed large $B \to K\eta'$ rates are naturally explained in QCDF without invoking, for example, significant flavor-singlet contributions or an enhanced hadronic matrix element $\langle 0|\bar{s}\gamma_5 s|\eta'\rangle$. Data on $B \to K\eta$ modes are also well accounted for by QCDF.

The values of the parameters $\alpha_4(K^{(*)}\eta_{q,s})$ and $\alpha_4(\eta_q K^{(*)})$ are given by

$$\begin{aligned} \alpha_4(K\eta_s) &= -0.098 - 0.013i, \\ \alpha_4(\eta_q K) &= -0.094 - 0.013i, \\ \alpha_4(K^*\eta_s) &= 0.035 - 0.0009i, \\ \alpha_4(\eta_q K^*) &= -0.036 - 0.0085i. \end{aligned} \qquad (12)$$

The magnitude of $\alpha_4(\eta_q K^*)$ is smaller than $\alpha_4(\eta_q K)$ owing to the smallness of $r_\chi^{K^*} \sim 0.36$ compared to $r_\chi^K \sim 1.45$ at the scale $\mu = 4.2$ GeV, while the smallness of $\alpha_4(K^*\eta_s)$ relative to $\alpha_4(K\eta_s)$ is due to the destructive interference in the former. The sign difference between $\alpha_4(\eta_q K^*)$ and $\alpha_4(K^*\eta_s)$ explains why $\Gamma(B \to K^*\eta) \gg \Gamma(B \to K^*\eta')$. Although the rates of $K^*\eta'$ and $K\eta$ are comparable, $\mathcal{B}(B \to K^*\eta)$ is much smaller than $\mathcal{B}(B \to K\eta')$.

The QCDF prediction for the branching fraction of $B \to K^*\eta'$, of order 1.5×10^{-6},[1] is smaller than the predictions of perturbative QCD (pQCD) and soft-collinear effective theory (SCET), but it is consistent with experiment within errors. The experimental values quoted in Table III are the *BABAR* measurements [1]. Belle obtained only the upper bounds: $\mathcal{B}(B^- \to K^{*-}\eta') < 2.9 \times 10^{-6}$ and $\mathcal{B}(\bar{B}^0 \to \bar{K}^{*0}\eta') < 2.6 \times 10^{-6}$ [14]. Therefore, although our central values are smaller than *BABAR*, they are consistent with

---

[1]The predictions $\mathcal{B}(B^- \to K^{*-}\eta') = 2.2 \times 10^{-6}$ and $\mathcal{B}(\bar{B}^0 \to \bar{K}^{*0}\eta') = 1.9 \times 10^{-6}$ obtained by Beneke and Neubert [8] in the so-called "S4" scenario in which power corrections to penguin annihilation are taken into account are consistent with ours.

TABLE III. Branching fractions (top, in units of 10^{-6}) and direct CP asymmetries (bottom, in units of percent) of $B \to (K, K^*) \times (\eta, \eta^{\prime})$ decays obtained in various approaches. The pQCD results are taken from [10] for $B \to K\eta^{(\prime)}$ with partial NLO corrections and from [11] for $B \to K^*\eta^{(\prime)}$. There are two solution sets with SCET predictions for decays involving η and/or $\eta^{\prime}$ [12,13]. The theoretical errors correspond to the uncertainties due to the variation of (i) Gegenbauer moments, decay constants, quark masses, form factors, the λ_B parameter for the B meson wave function, and (ii) $\rho_{A,H}$, $\phi_{A,H}$, respectively.

Mode	QCDF (this work)	pQCD	SCET	Expt. [1,2]
$B^- \to K^- \eta$	$2.2^{+1.7+1.1}_{-1.0-0.9}$	$3.2^{+1.2+2.7+1.1}_{-0.9-1.2-1.0}$	$2.7 \pm 4.8 \pm 0.4 \pm 0.3$ $2.3 \pm 4.5 \pm 0.4 \pm 0.3$	2.36 ± 0.27
$B^- \to K^- \eta^{\prime}$	$74.5^{+57.9+25.6}_{-25.3-19.0}$	$51.0^{+13.5+11.2+4.2}_{-8.2-6.2-3.5}$	$69.5 \pm 27.0 \pm 4.4 \pm 7.7$ $69.3 \pm 26.0 \pm 7.1 \pm 6.3$	71.1 ± 2.6
$\bar{B}^0 \to \bar{K}^0 \eta$	$1.5^{+1.4+0.9}_{-0.8-0.7}$	$2.1^{+0.8+2.3+1.0}_{-0.6-1.0-0.9}$	$2.4 \pm 4.4 \pm 0.2 \pm 0.3$ $2.3 \pm 4.4 \pm 0.2 \pm 0.5$	$1.12^{+0.30}_{-0.28}$
$\bar{B}^0 \to \bar{K}^0 \eta^{\prime}$	$70.9^{+54.1+24.2}_{-23.8-18.0}$	$50.3^{+11.8+11.1+4.5}_{-8.2-6.2-2.7}$	$63.2 \pm 24.7 \pm 4.2 \pm 8.1$ $62.2 \pm 23.7 \pm 5.5 \pm 7.2$	66.1 ± 3.1
$B^- \to K^{*-} \eta$	$15.8^{+8.2+9.6}_{-4.2-7.3}$	$22.13^{+0.26}_{-0.27}$	$17.9^{+5.5+3.5}_{-5.4-2.9}$ $18.6^{+4.5+2.5}_{-4.8-2.2}$	19.3 ± 1.6
$B^- \to K^{*-} \eta^{\prime}$	$1.6^{+2.1+3.7}_{-0.3-1.6}$	6.38 ± 0.26	$4.5^{+6.6+0.9}_{-3.9-0.8}$ $4.8^{+5.3+0.8}_{-3.7-0.6}$	$4.8^{+1.8a}_{-1.6}$
$\bar{B}^0 \to \bar{K}^{*0} \eta$	$15.7^{+7.7+9.6}_{-4.0-7.3}$	$22.31^{+0.28}_{-0.29}$	$16.6^{+5.1+3.2}_{-5.0-2.7}$ $16.5^{+4.1+2.3}_{-4.3-2.0}$	15.9 ± 1.0
$\bar{B}^0 \to \bar{K}^{*0} \eta^{\prime}$	$1.5^{+1.8+3.5}_{-0.3-1.6}$	$3.35^{+0.29}_{-0.27}$	$4.1^{+6.2+0.9}_{-3.6-0.7}$ $4.0^{+4.7+0.7}_{-3.4-0.6}$	$3.1^{+1.0b}_{-0.9}$
$B^- \to K^- \eta$	$-14.5^{+10.3+15.5}_{-26.0-10.7}$	$-11.7^{+6.8+3.9+2.9}_{-9.6-4.2-5.6}$	$33 \pm 30 \pm 7 \pm 3$ $-33 \pm 39 \pm 10 \pm 4$	-37 ± 9
$B^- \to K^- \eta^{\prime}$	$0.45^{+0.69+1.20}_{-0.55-0.98}$	$-6.2^{+1.2+1.3+1.3}_{-1.1-1.0-1.0}$	$-10 \pm 6 \pm 7 \pm 5$ $0.7 \pm 0.5 \pm 0.2 \pm 0.9$	$1.3^{+1.6}_{-1.7}$
$\bar{B}^0 \to \bar{K}^0 \eta$	$-23.6^{+9.8+12.6}_{-26.2-12.5}$	$-12.7^{+4.1+3.2+3.2}_{-4.1-1.5-6.7}$	$21 \pm 20 \pm 4 \pm 3$ $-18 \pm 22 \pm 6 \pm 4$	
$\bar{B}^0 \to \bar{K}^0 \eta^{\prime}$	$3.0^{+0.6+0.8}_{-0.5-0.8}$	$2.3^{+0.5+0.3+0.2}_{-0.4-0.6-0.1}$	$11 \pm 6 \pm 12 \pm 2$ $-27 \pm 7 \pm 8 \pm 5$	5 ± 5
$B^- \to K^{*-} \eta$	$-10.1^{+3.9+6.5}_{-3.7-7.8}$	$-24.57^{+0.72}_{-0.27}$	$-2.6^{+5.4+0.3}_{-5.5-0.3}$ $-1.9^{+3.4+0.1}_{-3.6-0.1}$	2 ± 6
$B^- \to K^{*-} \eta^{\prime}$	$69.7^{+6.5+27.9}_{-38.6-49.5}$	$4.60^{+1.16}_{-1.32}$	$2.7^{+27.4+0.4}_{-19.5-0.3}$ $2.6^{+26.7+0.2}_{-32.9-0.2}$	-26 ± 27
$\bar{B}^0 \to \bar{K}^{*0} \eta$	$3.4^{+0.4+2.7}_{-0.4-2.4}$	0.57 ± 0.011	$-1.1^{+2.3+0.1}_{-2.4-0.1}$ $-0.7^{+1.2+0.1}_{-1.3-0.0}$	19 ± 5
$\bar{B}^0 \to \bar{K}^{*0} \eta^{\prime}$	$8.8^{+8.8+30.8}_{-10.7-24.1}$	-1.30 ± 0.08	$9.6^{+8.9+1.3}_{-11.0-1.2}$ $9.9^{+6.2+0.9}_{-4.3-0.9}$	2 ± 23

[a]This is from the *BABAR* data [1]. Belle obtained an upper limit 2.9×10^{-6} [14].
[b]This is from the *BABAR* data [1]. Belle obtained an upper limit 2.6×10^{-6} [14].

Belle. It is very important to measure them to discriminate between various model predictions.

B. *CP* asymmetries

There are two modes in which direct CP asymmetries have been measured with significance around 4σ: $A_{CP}(K^- \eta) = -0.37 \pm 0.09$ and $A_{CP}(\bar{K}^{*0} \eta) = 0.19 \pm 0.05$. It is crucial to understand them. Since the two penguin diagrams in Figs. 1(b) and 1(c) contribute destructively to $B \to K\eta$ due to the opposite sign of f_{η}^q and f_{η}^s, the penguin amplitude is comparable in magnitude to the tree amplitude induced from $b \to u s\bar{u}$, contrary to the decay $B \to K\eta^{\prime}$ which is dominated by large penguin amplitudes.

Consequently, a sizable direct CP asymmetry is expected in $B^- \to K^- \eta$ but not in $K^- \eta^{\prime}$ [15].

In the absence of any power corrections, it appears that the QCDF prediction $A_{CP}(K^- \eta) = -0.233^{+0.164}_{-0.193}$ obtained in the leading $1/m_b$ expansion already agrees well with the data.[2] However, this agreement is just an accident. Recall that when power corrections are turned off, the predicted CP asymmetries for the penguin-dominated modes $K^- \pi^+$, $K^{*-} \pi^+$, $K^- \rho^+$, $K^- \rho^0$, and tree-dominated modes $\pi^+ \pi^-$, $\rho^\pm \pi^\mp$, and $\rho^- \pi^+$ are wrong in signs when confronted with experiment [5,6]. That is why it is important to con-

---

[2]Beneke and Neubert [8] obtained $A_{CP}(K^- \eta) = -0.189^{+0.290}_{-0.300}$ in their default predictions.

sider the effects of power corrections step by step. The QCDF results in the heavy quark limit should not be considered as the final QCDF predictions to be compared with experiment. It turns out that the aforementioned wrong signs can be flipped into the right direction by the power corrections from penguin annihilation.

However, a scrutiny of the QCDF predictions reveals more puzzles with respect to direct CP violation. While the signs of CP asymmetries in $K^-\pi^+$, $K^-\rho^0$ modes, etc., are flipped to the right ones in the presence of power corrections from penguin annihilation, the signs of A_{CP} in $B^- \to K^-\pi^0$, $K^-\eta$, $\pi^-\eta$ and $\bar{B}^0 \to \pi^0\pi^0$, $\bar{K}^{*0}\eta$ will also get reversed in such a way that they disagree with experiment [5,6]. Specifically, $A_{CP}(K^-\eta)$ is found to be of order 0.11 in the presence of penguin annihilation and hence it has a wrong sign. These CP puzzles can be resolved by having soft corrections to the color-suppressed tree coefficient a_2 so that a_2 is large and complex. When ρ_C and ϕ_C are turned on (see Eq. (11) with $\rho_C = 1.3$ and $\phi_C = -70°$ [5]), $A_{CP}(K^-\eta)$ will be reduced to -0.02 if there is no intrinsic charm content of the η. Although the decay constant $f^c_\eta \approx -2$ MeV is much smaller than $f^{q,s}_\eta$ [see Eq. (A12)], its effect is Cabibbo-Kobayashi-Maskawa (CKM) enhanced by $V_{cb}V^*_{cs}/(V_{ub}V^*_{us})$. Therefore, the charm content of the η may have a significant impact on CP violation. Indeed, when f^c_η is turned on, $A_{CP}(K^-\eta)$ finally reaches the level of -15% with a sign in agreement with experiment. Hence, CP asymmetry in $B^- \to K^-\eta$ is the place where the charm content of the η plays a role.[3] The pQCD prediction is similar to QCDF. For comments on the pQCD calculation of $A_{CP}(K^-\eta)$, the reader is referred to [5]. Note that while both QCDF and pQCD lead to a correct sign for $A_{CP}(K^-\eta)$, the predicted magnitude still falls short of the measurement -0.37 ± 0.09.

As for CP asymmetry in $\bar{B}^0 \to \bar{K}^{*0}\eta$, we have $A_{CP}(\bar{K}^{*0}\eta) = (3.1^{+2.0}_{-1.9})\%$ in the heavy quark limit. It is modified to $(0.12^{+2.10}_{-1.60})\%$ by penguin annihilation. Soft corrections to the color-suppressed tree amplitude is needed to improve the prediction and finally we obtain $A_{CP}(\bar{K}^{*0}\eta) = (3.4^{+2.8}_{-2.4})\%$ (Table III). Unlike the $K^0\eta$ mode, the charm content of the η here does not play an essential role for CP violation in $K^{*0}\eta$. We see from Table III that QCDF is in better agreement with experiment than pQCD and SCET, though it is still smaller than the data.

IV. $B \to K^*_0(1430)\eta^{(')}$ DECAYS IN QCDF

The hadronic charmless B decays into a scalar meson and a pseudoscalar meson have been studied in QCDF in

---

[3]One of us (C. K. C.) has studied residual final-state interaction effects in charmless B decays [9]. In this approach, $A_{CP}(K^-\eta)$ of order -0.27 can be induced through the decay $B^- \to K^-\eta'$ followed by $K^-\eta' \to K^-\eta$ rescattering via penguin diagrams. This rescattering mimics the effect of the charm content in the η.

[16]. For scalar mesons above 1 GeV we have explored two possible scenarios in the QCD sum rule method, depending on whether the light scalars κ, $a_0(980)$, and $f_0(980)$ are treated as the lowest-lying $q\bar{q}$ states or 4-quark particles: (i) In scenario 1, we treat κ, $a_0(980)$, $f_0(980)$ as the lowest-lying states, and $K^*_0(1430)$, $a_0(1450)$, $f_0(1500)$ as the corresponding first excited states, respectively, and (ii) we assume in scenario 2 that $K^*_0(1430)$, $a_0(1450)$, $f_0(1500)$ are the lowest-lying resonances and the corresponding first excited states lie between (2.0–2.3) GeV. Scenario 2 corresponds to the case that light scalar mesons are 4-quark bound states, while all scalar mesons are made of two quarks in scenario 1. We found that scenario 2 is preferable. Indeed, lattice calculations have confirmed that $a_0(1450)$ and $K^*_0(1430)$ are lowest-lying P-wave $q\bar{q}$ mesons [17], and suggested that σ and κ are S-wave tetra-quark mesonia [17,18].

Decay constants of scalar mesons are defined as

$$\langle S(p)|\bar{q}_2\gamma_\mu q_1|0\rangle = f_S p_\mu, \qquad \langle S|\bar{q}_2 q_1|0\rangle = m_S\bar{f}_S. \tag{13}$$

The vector decay constant f_S and the scale-dependent scalar decay constant $\bar{f}_S$ are related by equations of motion

$$\mu_S f_S = \bar{f}_S, \quad \text{with} \quad \mu_S = \frac{m_S}{m_2(\mu) - m_1(\mu)}, \tag{14}$$

where m_2 and m_1 are the running current quark masses and m_S is the scalar meson mass. In general, the twist-2 light-cone distribution amplitude (LCDA) of the scalar meson Φ_S has the form

$$\Phi_S(x, \mu) = f_S 6x(1 - x)$$
$$\times \left[1 + \mu_S \sum_{m=1}^\infty B_m(\mu)C^{3/2}_m(2x - 1)\right], \tag{15}$$

where B_m are Gegenbauer moments and $C^{3/2}_m$ are the Gegenbauer polynomials. For twist-3 LCDAs, we use

$$\Phi^s_S(x) = \bar{f}_S, \qquad \Phi^\sigma_S(x) = \bar{f}_S 6x(1 - x). \tag{16}$$

Since $\mu_S \equiv 1/B_0 \gg 1$ and even Gegenbauer coefficients are suppressed, it is clear that the LCDA of the scalar meson is dominated by the odd Gegenbauer moments. In contrast, the odd Gegenbauer moments vanish for the π and ρ mesons. The Gegenbauer moments B_1, B_3, and the scalar decay constant $\bar{f}_{K^*_0}$ in scenarios 1 and 2 obtained using the QCD sum rule method [16] are listed in Table IV.

Form factors for $B \to S$ transitions are defined by

$$\langle S(p')|A_\mu|B(p)\rangle = -i\left[\left(P_\mu - \frac{m^2_B - m^2_S}{q^2}q_\mu\right)F^{BS}_1(q^2)\right.$$
$$\left. + \frac{m^2_B - m^2_S}{q^2}q_\mu F^{BS}_0(q^2)\right], \tag{17}$$

where $P_\mu = (p + p')_\mu$, $q_\mu = (p - p')_\mu$. As shown in [19], a factor of $(-i)$ is needed in $B \to S$ transition in order to obtain positive $B \to S$ form factors. This also can

TABLE IV.   Gegenbauer moments B_1, B_3 and the scalar decay constant $\bar{f}_{K_0^*}$ (in units of MeV) in scenario 1 and scenario 2 at the scales $\mu = 1$ GeV and 2.1 GeV (shown in parentheses) obtained using the QCD sum-rule method [16].

	B_1	B_3	$\bar{f}_{K_0^*}$
Scenario 1	$0.58 \pm 0.07(0.39 \pm 0.05)$	$-1.20 \pm 0.08(-0.70 \pm 0.05)$	$-300 \pm 30(-370 \pm 35)$
Scenario 2	$-0.57 \pm 0.13(-0.39 \pm 0.09)$	$-0.42 \pm 0.22(-0.25 \pm 0.13)$	$445 \pm 50(550 \pm 60)$

be checked from heavy quark symmetry [19]. As a consequence, the factorizable amplitudes $X^{(BP,S)}$ and $X^{(BS,P)}$ defined in Eq. (4) are of opposite sign. In this work we shall use the form factors[4]

$$F_0^{BK_0^*}(q^2) = \frac{0.21}{1 - 0.59(q^2/m_B^2) + 0.09(q^4/m_B^4)} \quad (18)$$

in scenario 1 and

$$F_0^{BK_0^*}(q^2) = \frac{0.26}{1 - 0.44(q^2/m_B^2) + 0.05(q^4/m_B^4)} \quad (19)$$

in scenario 2. They are obtained using the covariant light-front quark model [19].

For the convenience of ensuing discussions, we would write

$$A_{B \to K_0^* \eta} = X^{(BK_0^*, \eta_q)}C_1 + X^{(BK_0^*, \eta_s)}C_2 + X^{(B\eta_q, K_0^*)}C_3,$$
$$A_{B \to K_0^* \eta'} = X^{(BK_0^*, \eta_q')}C_1 + X^{(BK_0^*, \eta_s')}C_2 + X^{(B\eta_q', K_0^*)}C_3,$$
$$(20)$$

where C_1, C_2, and C_3 terms correspond to Figs. 1(a)–1(c), respectively. The expressions of C_i's in terms of the parameters α_i^p can be found in Eq. (3). As noticed in [16], the pattern of a_i or α_i in $B \to SP$ decays (see Table V) can be quite different from that in PP modes. For example, we have

$$\alpha_2(K\eta_{q,s}) = 0.21 - 0.08i,$$
$$\alpha_3(K\eta_{q,s}) = -0.010 - 0.0058i,$$
$$\alpha_4^c(K\eta_q) = -0.073 - 0.011i, \quad (21)$$
$$\alpha_4^c(K\eta_s) = -0.098 - 0.013i,$$
$$\alpha_4^c(\eta_q K) = -0.094 - 0.013i,$$

for $K\eta^{(\prime)}$ modes. Since the chiral factor $r_\chi^{K_0^*} = 12.3$ at $\mu = 4.2$ GeV is larger than $r_\chi^K = 1.5$ by 1 order of magnitude owing to the large mass of $K_0^*(1430)$, it follows that $\alpha_4^c(\eta_q K_0^*)$ is much greater than $\alpha_4^c(K_0^* \eta_s)$ and $\alpha_4^c(K_0^* \eta_q)$. Likewise, the real part of $\alpha_{2,3}(K_0^* \eta_{q,s})$ is greater than that of $\alpha_{2,3}(K\eta_{q,s})$ because the hard spectator term $H(M_1 M_2)$

---

[4]In footnote 9 of [16], we have emphasized that the decay constant and the form factor for the excited state are of opposite sign. Hence, we do not agree with [10,20] on the sign of $F_0^{BK_0^*}$ in scenario 1.

$$H(M_1 M_2) = \frac{if_B f_{M_1} f_{M_2}}{X^{(\bar{B}M_1, M_2)}} \frac{m_B}{\lambda_B} \int_0^1 dx dy \left(\frac{\Phi_{M_1}(x)\Phi_{M_2}(y)}{(1-x)(1-y)} \right.$$
$$\left. + r_\chi^{M_1} \frac{\Phi_{m_1}(x)\Phi_{M_2}(y)}{(1-x)y} \right), \quad (22)$$

with Φ_M and Φ_m being the twist-2 and twist-3 LCDAs of the meson M, respectively, is greatly enhanced for $M_1 = K_0^*(1430)$ due to the large chiral factor $r_\chi^{K_0^*}$.

Because of the small vector decay constant of $K_0^*(1430)$, $X^{(B\eta_q^{(\prime)}, K_0^*)}$ is suppressed relative to $X^{(BK_0^*, \eta_q^{(\prime)})}$ and $X^{(BK_0^*, \eta_s^{(\prime)})}$. However, C_3 gains a large enhancement from $\alpha_4^c(\eta_q K_0^*)$. As a result, the amplitude of Fig. 1(c) is comparable to that of Fig. 1(a). The decay pattern of $B \to K_0^* \eta^{(\prime)}$ depends on whether the scalar meson $K_0^*(1430)$ is an excited state of κ or a lowest-lying P-wave $q\bar{q}$ state. In scenario 1, we have (in units of GeV^3)

$$X^{(BK_0^*, \eta_q)} = -0.60, \qquad X^{(BK_0^*, \eta_s)} = 0.61,$$
$$X^{(B\eta_q, K_0^*)} = -0.15, \qquad X^{(BK_0^*, \eta_q')} = -0.49, \quad (23)$$
$$X^{(BK_0^*, \eta_s')} = -0.75, \qquad X^{(B\eta_q', K_0^*)} = -0.12.$$

Consequently, Fig. 1(b) interferes destructively (constructively) with Figs. 1(a) and 1(c) for $K_0^* \eta$ ($K_0^* \eta'$). This leads to $\mathcal{B}(B \to K_0^* \eta') \gg \mathcal{B}(B \to K_0^* \eta)$ (see Table VI), which is in sharp disagreement with experiment.

The decay pattern in scenario 2 is quite different. Because of the large magnitude of $\alpha_3(K_0^* \eta_{q,s})$ and the large cancellation between $\alpha_3(K_0^* \eta_s)$ and $\alpha_4(K_0^* \eta_s)$ in C_2, $B \to K_0^* \eta^{(\prime)}$ decays are dominated by the contributions from Figs. 1(a) and 1(c), contrary to the $B \to K^{(*)} \eta^{(\prime)}$ decays which are governed by Figs. 1(b) and 1(c). Numerically, we obtain

$$C_1 = -0.098 + 0.011i, \qquad C_3 = 0.455 + 0.017i,$$
$$X^{(B\eta_q, K_0^*)} = 0.22, \qquad X^{(BK_0^*, \eta_q)} = -0.74, \quad (24)$$
$$X^{(BK_0^*, \eta_q')} = -0.60, \qquad X^{(B\eta_q', K_0^*)} = 0.18.$$

Therefore, the penguin diagrams in Figs. 1(a) and 1(c) contribute constructively to both $K_0^* \eta$ and $K_0^* \eta'$ with comparable magnitudes. Since $X^{(BK_0^*, \eta_q)}/X^{(BK_0^*, \eta_q')} = X^{(B\eta_q, K_0^*)}/X^{(B\eta_q', K_0^*)} = \cot\phi \approx 1.23$, it is clear that $A_{B \to K_0^* \eta}/A_{B \to K_0^* \eta'} \approx \cot\phi$ and hence $B \to K_0^* \eta$ should have a rate larger than $B \to K_0^* \eta'$ in scenario 2 as the mixing angle ϕ is less than $45°$.

TABLE V. Values of $\alpha_{2,3,4}$ at $\mu = 4.2$ GeV in scenarios 1 and 2.

	$\alpha_2(K_0^*\eta_{q,s})$	$\alpha_3(K_0^*\eta_{q,s})$	$\alpha_4^c(K_0^*\eta_s)$	$\alpha_4^c(K_0^*\eta_q)$	$\alpha_4^c(\eta_q K_0^*)$
Scenario 1	$-0.27 - 0.08i$	$0.050 + 0.006i$	$0.025 + 0.001i$	$0.0001 - 0.0017i$	$0.50 + 0.09i$
Scenario 2	$0.51 - 0.08i$	$-0.047 + 0.006i$	$0.043 + 0.009i$	$0.018 - 0.002i$	$0.45 + 0.02i$

The QCDF results for branching fractions and *CP* asymmetries of $B \to K_0^*(1430)\eta^{(')}$ obtained in two different scenarios are shown in Table VI where the central values are for $\rho_A = \rho_C = 0$ and $\phi_A = \phi_C = 0$ and the ranges $0 \le \rho_{A,H} \le 0.5$ and $0 \le \phi_{A,H} \le 2\pi$ have been considered for the estimate of uncertainties. It is evident that scenario 2 is in better agreement with experiment than scenario 1. This implies that the scalar meson $K_0^*(1430)$ is a lowest-lying rather than excited $q\bar{q}$ state.

Several remarks are in order. (i) If $X^{(BK_0^*, \eta_q)}$ and $X^{(B\eta_q, K_0^*)}$ are of the same sign, the interference between the C_1 and C_3 terms will become destructive in scenario 2 and yield too small rates for both $K_0^*\eta$ and $K_0^*\eta'$. (ii) A recent pQCD calculation [10] indicates that $\mathcal{B}(B \to K_0^*\eta')/\mathcal{B}(B \to K_0^*\eta) \approx 2$ in scenario 1 and $\mathcal{B}(B \to K_0^*\eta') \approx 75 \times 10^{-6}$ in scenario 2. Neither of them is consistent with experiment. (iii) Different estimates of form factors at $q^2 = 0$ were obtained recently: $F_0^{BK_0^*}(0) \sim -0.34$ [20], -0.44 [10] in scenario 1, and $F_0^{BK_0^*}(0) \sim 0.60$ [20], 0.76 [10] in scenario 2. If these form factors are used in QCDF calculations, we will have $\mathcal{B}(B \to K_0^*\eta) \sim 22 \times 10^{-6} \gg \mathcal{B}(B \to K_0^*\eta') \sim 1 \times 10^{-6}$ in scenario 2 for $F_0^{BK_0^*}(0) = 0.60$ as an example. This implies that a small form factor for $B \to K_0^*(1430)$ transition is preferable.

V. $B \to K_2^*(1430)\eta^{(')}$ IN NAIVE FACTORIZATION

The observed $J^P = 2^+$ tensor mesons $f_2(1270)$, $f_2'(1525)$, $a_2(1320)$, and $K_2^*(1430)$ form an SU(3) 1^3P_2 nonet. The $q\bar{q}$ content for isodoublet and isovector tensor resonances is obvious. The polarization tensor $\varepsilon_{\mu\nu}$ of a $^3P_2$ tensor meson with $J^{PC} = 2^{++}$ satisfies the relations

$$\varepsilon_{\mu\nu} = \varepsilon_{\nu\mu}, \qquad \varepsilon_\mu^\mu = 0, \qquad p_\mu \varepsilon^{\mu\nu} = p_\nu \varepsilon^{\mu\nu} = 0,$$

(25)

where p^μ is the momentum of the tensor meson. Therefore,

$$\langle 0|(V - A)_\mu|T(\varepsilon, p)\rangle = a\varepsilon_{\mu\nu}p^\nu + b\varepsilon_\nu^\nu p_\mu = 0, \quad (26)$$

and hence the decay constant of the tensor meson vanishes identically; that is, the tensor meson cannot be produced from the $V - A$ current. This means that Fig. 1(c) does not contribute to $B \to K_2^*\eta^{(')}$ under the factorization hypothesis.

The general expression for the $B \to T$ transition has the form [22]

TABLE VI. Branching fractions (top, in units of 10^{-6}) and direct *CP* asymmetries (bottom, in units of percent) of $B \to K_0^*(1430)(\eta, \eta')$ decays obtained in QCDF (this work) and pQCD [21] in scenario 1 (first entry) and scenario 2 (second entry).

Mode	QCDF (this work)	pQCD	Expt. [1,2]
$B^- \to K_0^{*-}(1430)\eta$	$0.5^{+1.7+11.9}_{-0.4-0.5}$ $13.3^{+6.2+48.6}_{-3.6-10.1}$	$11.8^{+5.3+0.3+1.1+2.5}_{-3.5-0.4-1.2-2.3}$ $33.8^{+13.5+1.1+7.7+8.2}_{-9.0-1.1-7.0-7.3}$	15.8 ± 3.1
$B^- \to K_0^{*-}(1430)\eta'$	$27.8^{+20.8+14.1}_{-10.2-17.6}$ $9.6^{+12.9+10.0}_{-6.1-9.4}$	$21.6^{+1.6+3.1+4.0+4.5}_{-0.5-2.8-3.6-4.1}$ $77.5^{+15.8+6.2+21.0+18.0}_{-10.8-5.8-16.5-16.1}$	5.2 ± 2.1
$\bar{B}^0 \to \bar{K}_0^{*0}(1430)\eta$	$0.4^{+1.5+11.8}_{-0.3-0.4}$ $12.6^{+5.7+50.1}_{-3.4-9.3}$	$9.1^{+4.4+0.0+1.1+2.0}_{-2.8-0.1-1.1-1.8}$ $28.4^{+11.6+1.4+6.4+6.9}_{-7.8-1.4-5.9-6.2}$	9.6 ± 1.9
$\bar{B}^0 \to \bar{K}_0^{*0}(1430)\eta'$	$26.6^{+19.7+17.3}_{-9.8-16.5}$ $8.7^{+11.7+7.5}_{-5.5-3.1}$	$22.0^{+1.6+3.2+3.9+4.6}_{-0.5-3.6-3.0-4.2}$ $74.2^{+15.0+6.4+20.5+17.2}_{-10.3-5.7-16.2-15.5}$	6.3 ± 1.6
$B^- \to K_0^{*-}(1430)\eta$	$8.3^{+21.1+11.7}_{-5.4-11.7}$ $1.7^{+0.2+2.4}_{-0.2-2.4}$		5 ± 13
$B^- \to K_0^{*-}(1430)\eta'$	$-0.3^{+0.2+0.4}_{-0.2-0.4}$ $1.2^{+0.7+1.7}_{-0.6-1.7}$		6 ± 20
$\bar{B}^0 \to \bar{K}_0^{*0}(1430)\eta$	$14.5^{+36.3+20.4}_{-10.8-20.4}$ $2.2^{+0.2+3.1}_{-0.2-3.1}$		6 ± 13
$\bar{B}^0 \to \bar{K}_0^{*0}(1430)\eta'$	$-0.2^{+0.1+0.3}_{-0.1-0.3}$ $1.1^{+0.5+1.6}_{-0.5-1.6}$		-19 ± 17

TABLE VII. Parameters for the $B \to K_2^*(1430)$ transition form factors obtained in the covariant light-front model [19]. The form factor k is dimensionless, while k, b_+, and b_- are in units of GeV^{-2}. The numbers in parentheses are the form factors at $q^2 = 0$ obtained using the ISGW2 model [23].

F	$F(0)$	a	b	F	$F(0)$	a	b
$h^{BK_2^*}$	0.008 (0.016)	2.17	2.22	$k^{BK_2^*}$	0.015 (0.293)	-3.70	1.78
$b_+^{BK_2^*}$	$-0.006(-0.006)$	1.96	1.79	$b_-^{BK_2^*}$	0.002 (0.0063)	0.38	0.92

$$\langle T(\varepsilon, p_T)|(V-A)_\mu|B(p_B)\rangle$$
$$= ih(q^2)\epsilon_{\mu\nu\rho\sigma}\varepsilon^{*\nu\alpha}p_{B\alpha}(p_B + p_T)^\rho(p_B - p_T)^\sigma$$
$$+ k(q^2)\varepsilon_{\mu\nu}^* p_B^\nu + b_+(q^2)\varepsilon_{\alpha\beta}^* p_B^\alpha p_B^\beta(p_B + p_T)_\mu$$
$$+ b_-(q^2)\varepsilon_{\alpha\beta}^* p_B^\alpha p_B^\beta(p_B - p_T)_\mu. \qquad (27)$$

The form factors h, k, b_+, and b_- have been calculated in the Isgur-Scora-Grinstein-Wise (ISGW) quark model [22] and its improved version, the ISGW2 model [23]. They have also been computed in the covariant light-front (CLF) quark model [19] and are listed in Table VII for form factors fitted to a 3-parameter form

$$F(q^2) = \frac{F(0)}{1 - a(q^2/m_B^2) + b(q^2/m_B^2)^2}. \qquad (28)$$

Notice that when q^2 increases, $h(q^2)$, $b_+(q^2)$, and $b_-(q^2)$ increase more rapidly in the CLF model than in the ISGW2 model and that the form factor k in both models is quite different.

The decay amplitude of $B \to TP$ always has the generic expression

$$A(B \to TP) = \varepsilon_{\mu\nu}^* p_B^\mu p_B^\nu M(B \to TP). \qquad (29)$$

The decay rate is given by

$$\Gamma(B \to TP) = \frac{p_c^5}{12\pi m_T^2}\left(\frac{m_B}{m_T}\right)^2 |M(B \to TP)|^2, \qquad (30)$$

where p_c is the magnitude of the 3-momentum of either final-state meson in the rest frame of the B meson. Since the QCDF approach for $B \to TP$ has not been developed, we will reply on naive factorization to make estimates; that is, we will not include vertex, hard spectator, and penguin corrections in Eq. (8) for the calculation of a_i.

The predictions of $B \to K_2^*(1430)\eta^{(\prime)}$ in various models are shown in Table VIII. We see that the predicted rates in naive factorization are too small by 1 order of magnitude.[5] It was found in [24] that $\mathcal{B}(B \to K_2^*\eta')/\mathcal{B}(B \to K_2^*\eta) \sim 45$, a prediction not borne out by experiment. This is ascribed to the fact that the matrix element

$$\langle \eta'|\bar{s}\gamma_5 s|0\rangle = -i\frac{m_{\eta'}^2}{2m_s}f_{\eta'}^s, \qquad (31)$$

used in [24] is erroneous as it does not have the correct chiral behavior in the chiral limit; the SU(3)-singlet η_1 acquires a mass of the QCD anomaly which does not vanish in the chiral limit. Applying the anomalous equation of motion Eq. (A7) and neglecting the masses of u and d quarks, one gets [27,28]

$$\langle \eta^{(\prime)}|\bar{s}\gamma_5 s|0\rangle = -i\frac{m_{\eta^{(\prime)}}^2}{2m_s}\left(f_{\eta^{(\prime)}}^s - \frac{1}{\sqrt{2}}f_{\eta^{(\prime)}}^q\right). \qquad (32)$$

Since $f_{\eta'}^q/\sqrt{2}$ is about half of $f_{\eta'}^s$, this means that the η' matrix element of the pseudoscalar density is reduced roughly by a factor of 2. On the contrary, the η matrix element is enhanced owing to the opposite sign of f_η^q and f_η^s. A rigorous result without neglecting light quark masses is $\langle \eta^{(\prime)}|\bar{s}\gamma_5 s|0\rangle = -ih_{\eta^{(\prime)}}^s/(2m_s)$ [cf. Eq. (A4)]. Since the magnitude of h_η^s is numerically close to $h_{\eta'}^s$ [see Eq. (A12)], it becomes clear that the rate of $K_2^*\eta$ is comparable to but slightly smaller than the $K_2^*\eta'$ one. Our results agree with [25] as we use the same form factors derived from the CLF model.[6] The predictions of [26] are too small as the authors only considered the tree diagram effects and neglected the important penguin contributions.

A slightly large rate of $K_2^*\eta'$ over $K_2^*\eta$ comes from two sources: (i) $|f_{\eta'}^s| > |f_\eta^s|$ and (ii) a destructive (constructive) interference between Figs. 1(a) and 1(b) for $K_2^*\eta$ ($K_2^*\eta'$). It is expected that $\Gamma(B \to K_2^*\eta')/\Gamma(B \to K_2^*\eta) \sim 2.5$. Since the predicted absolute rates are too small by 1 order of magnitude,[7] the discrepancy between theory and experiment may call for the study of (i) next-to-leading order (NLO) effects from vertex, hard spectator scattering, and penguin corrections; (ii) power corrections from penguin annihilation; and (iii) improved estimate of $B \to T$ form factors. The detailed investigation will be left to a future work.

---

[5]Although the form factor $k(q^2)$ is very different in the CLF and ISGW2 models, the magnitude of $F(q^2) = k(q^2) + (m_B^2 - m_T^2)b_+(q^2) + q^2b_-(q^2) = -0.15$ in the former and 0.14 in the latter for q^2 in the range between m_η^2 and $m_{\eta'}^2$ is about the same. Consequently, the predicted rates of $B \to K_2^*\eta^{(\prime)}$ are basically independent of the form-factor models.

[6]The only difference between our work and [25] is that we use Eq. (A4) for the $\eta^{(\prime)}$ matrix elements of pseudoscalar densities, while the authors of [25] use Eq. (32).

[7]The same issue also occurs in the $D \to TP$ system [29]. The predicted branching fractions based on factorization are at least 2 orders of magnitude smaller than data, even for decays free of weak annihilation contributions. We cannot find possible sources of rate enhancement.

TABLE VIII. Branching fractions (in units of 10^{-6}) of $B \to K_2^*(1430)(\eta, \eta')$ decays obtained in various approaches. The predictions of [24] are for $1/N_c^{\text{eff}} = 0.3$.

Mode	This work	Kim-Lee-Oh [24]	Munoz-Quintero [25]	Sharma-Verma [26]	Expt. [1,2]
$B^- \to K_2^{*-}(1430)\eta$	1.1	0.031	1.19	0.01	9.1 ± 3.0
$B^- \to K_2^{*-}(1430)\eta'$	2.7	1.4	2.70	0.007	$28.0^{+5.3}_{-5.0}$
$\bar{B}^0 \to \bar{K}_2^{*0}(1430)\eta$	1.0	0.029	1.09	0.01	9.6 ± 2.1
$\bar{B}^0 \to \bar{K}_2^{*0}(1430)\eta'$	2.5	1.3	2.46	0.006	$13.7^{+3.2}_{-3.1}$

VI. CONCLUSIONS

We have studied the decays $B \to K_h \eta$ and $B \to K_h \eta'$ within the framework of QCDF for $K_h = K, K^*, K_0^*(1430)$ and naive factorization for $K_h = K_2^*(1430)$. There are three different types of penguin contributions: (i) $b \to sq\bar{q} \to s\eta_q$, (ii) $b \to ss\bar{s} \to s\eta_s$, and (iii) $b \to sq\bar{q} \to q\bar{K}_h$, corresponding to Figs. 1(a)–1(c), respectively. Our conclusions are as follows:

(i) $B \to K^{(*)}\eta^{(')}$ decays are dominated by type-II and type-III penguin contributions. The interference, constructive for $K\eta'$ and $K^*\eta$ and destructive for $K\eta$ and $K^*\eta'$, between Figs. 1(b) and 1(c) explains the pattern of $\Gamma(B \to K\eta') \gg \Gamma(B \to K\eta)$ and $\Gamma(B \to K^*\eta') \ll \Gamma(B \to K^*\eta)$. Within QCDF, the observed large rate of the $K\eta'$ mode can be naturally explained without invoking flavor-singlet contributions or something exotic. The predicted central values of the decay rates for $K^{*-}\eta'$ and $K^{*0}\eta'$ are smaller than *BABAR* but consistent with Belle.

(ii) There are two $K^{(*)}\eta^{(')}$ modes in which direct *CP* asymmetries have been measured with significance around 4σ: $A_{CP}(K^-\eta) = -0.37 \pm 0.09$ and $A_{CP}(\bar{K}^{*0}\eta) = 0.19 \pm 0.05$. In QCDF, power corrections from penguin annihilation which are needed to resolve *CP* puzzles in $K^-\pi^+$ and $\pi^+\pi^-$ modes will flip $A_{CP}(K^-\eta)$ into a wrong sign. We show that soft corrections to the color-suppressed tree amplitude a_2 in conjunction with the charm content of the η will finally lead to $A_{CP}(K^-\eta) = -0.15^{+0.19}_{-0.28}$. Soft corrections to a_2 are also needed to improve the prediction for $A_{CP}(\bar{K}^{*0}\eta)$. The QCDF prediction is in better agreement with experiment than pQCD and SCET.

(iii) The decay pattern of $B \to K_0^*(1430)\eta^{(')}$ depends on whether $K_0^*(1430)$ is an excited state of κ or a lowest-lying P-wave $q\bar{q}$ state. If $K_0^*(1430)$ is an excited state of $q\bar{q}$, one will have a destructive (constructive) interference of Fig. 1(b) with Figs. 1(a) and 1(c) for $K_0^*\eta$ ($K_0^*\eta'$). This leads to $\mathcal{B}(B \to K_0^*\eta') \gg \mathcal{B}(B \to K_0^*\eta)$. If $K_0^*(1430)$ is made of the lowest-lying $q\bar{q}$, we found that Figs. 1(a) and 1(c) interfere constructively and that $A(B \to K_0^*\eta)/A(B \to K_0^*\eta') \approx \cot\phi$ with ϕ being the $\eta - \eta'$ mixing angle in the η_q, η_s flavor basis. Hence, $K_0^*\eta$ has a rate slightly larger than $K_0^*\eta'$ owing to the fact that ϕ is less than $45°$. The agreement of the latter scenario

with experiment indicates that the scalar meson $K_0^*(1430)$ is indeed a bound state of the low-lying $q\bar{q}$ state in P-wave.

(iv) Figure 1(c) does not contribute to $B \to K_2^*\eta^{(')}$ under the factorization hypothesis and Fig. 1(b) dominates. The ratio $\Gamma(B \to K_2^*\eta')/\Gamma(B \to K_2^*\eta)$ is expected to be of order 2.5 as a consequence of (i) $|f_{\eta'}^s| > |f_\eta^s|$ and (ii) a destructive (constructive) interference between Figs. 1(a) and 1(b) for $K_2^*\eta$ ($K_2^*\eta'$). However, the predicted rates of $B \to K_2^*\eta^{(')}$ in naive factorization are too small by 1 order of magnitude and this issue remains to be resolved.

APPENDIX: THE $\eta - \eta'$ SYSTEM

Decay constants $f_{\eta^{(')}}^q$, $f_{\eta^{(')}}^s$, and $f_{\eta^{(')}}^c$ are defined by

$$\langle 0|\bar{q}\gamma_\mu\gamma_5 q|\eta^{(')}\rangle = i\frac{1}{\sqrt{2}}f_{\eta^{(')}}^q p_\mu,$$
$$\langle 0|\bar{s}\gamma_\mu\gamma_5 s|\eta^{(')}\rangle = if_{\eta^{(')}}^s p_\mu, \quad \text{(A1)}$$
$$\langle 0|\bar{c}\gamma_\mu\gamma_5 c|\eta^{(')}\rangle = if_{\eta^{(')}}^c p_\mu,$$

while the widely studied decay constants f_q and f_s are defined as [3]

$$\langle 0|\bar{q}\gamma^\mu\gamma_5 q|\eta_q\rangle = \frac{i}{\sqrt{2}}f_q p^\mu,$$
$$\langle 0|\bar{s}\gamma^\mu\gamma_5 s|\eta_s\rangle = if_s p^\mu. \quad \text{(A2)}$$

The ansatz made by Feldmann, Kroll, and Stech (FKS) [3] is that the decay constants in the quark flavor basis follow the same pattern of $\eta - \eta'$ mixing given in Eq. (1)

$$\begin{pmatrix} f_\eta^q & f_\eta^s \\ f_{\eta'}^q & f_{\eta'}^s \end{pmatrix} = \begin{pmatrix} \cos\phi & -\sin\phi \\ \sin\phi & \cos\phi \end{pmatrix}\begin{pmatrix} f_q & 0 \\ 0 & f_s \end{pmatrix}. \quad \text{(A3)}$$

Empirically, this ansatz works very well [3]. Theoretically,

it has been shown recently that this assumption can be justified in the large-N_c approach [30].

Consider the matrix elements of pseudoscalar densities [31]

$$2m_q\langle 0|\bar{q}\gamma_5 q|\eta^{(\prime)}\rangle = \frac{i}{\sqrt{2}}h^q_{\eta^{(\prime)}},$$
$$2m_s\langle 0|\bar{s}\gamma_5 s|\eta^{(\prime)}\rangle = ih^s_{\eta^{(\prime)}}. \tag{A4}$$

One can define the parameters h_q and h_s in analogue to f_q and f_s,

$$2m_q\langle 0|\bar{q}\gamma_5 q|\eta_q\rangle = \frac{i}{\sqrt{2}}h_q, \qquad 2m_s\langle 0|\bar{s}\gamma_5 s|\eta_s\rangle = ih_s, \tag{A5}$$

and relate them to $h^{q,s}_{\eta,\eta'}$ by the same FKS ansatz

$$\begin{pmatrix} h^q_\eta & h^s_\eta \\ h^q_{\eta'} & h^s_{\eta'} \end{pmatrix} = \begin{pmatrix} \cos\phi & -\sin\phi \\ \sin\phi & \cos\phi \end{pmatrix}\begin{pmatrix} h_q & 0 \\ 0 & h_s \end{pmatrix}. \tag{A6}$$

Using the equations of motion

$$\partial_\mu(\bar{q}\gamma^\mu\gamma_5 q) = 2im_q\bar{q}\gamma_5 q + \frac{\alpha_s}{4\pi}G_{\mu\nu}\tilde{G}^{\mu\nu},$$
$$\partial_\mu(\bar{s}\gamma^\mu\gamma_5 s) = 2im_s\bar{s}\gamma_5 s + \frac{\alpha_s}{4\pi}G_{\mu\nu}\tilde{G}^{\mu\nu}, \tag{A7}$$

one can express all nonperturbative parameters in terms of the decay constants f_q, f_s, and the mixing angle ϕ:

$$h_q = f_q(m^2_\eta\cos^2\phi + m^2_{\eta'}\sin^2\phi)$$
$$\quad - \sqrt{2}f_s(m^2_{\eta'} - m^2_\eta)\sin\phi\cos\phi,$$
$$h_s = f_s(m^2_{\eta'}\cos^2\phi + m^2_\eta\sin^2\phi)$$
$$\quad - \frac{f_q}{\sqrt{2}}(m^2_{\eta'} - m^2_\eta)\sin\phi\cos\phi. \tag{A8}$$

For numerical calculations we shall use those parameters determined from a fit to experimental data [3]

$$f_q = (1.07 \pm 0.02)f_\pi, \qquad f_s = (1.34 \pm 0.06)f_\pi,$$
$$\phi = 39.3° \pm 1.0°. \tag{A9}$$

The masses of η_q and η_s read [3]

$$m^2_{\eta_q} = \frac{\sqrt{2}}{f_q}\langle 0|m_u\bar{u}i\gamma_5 u + m_d\bar{d}i\gamma_5 d|\eta_q\rangle$$
$$\quad + \frac{\sqrt{2}}{f_q}\langle 0|\frac{\alpha_s}{4\pi}G\tilde{G}|\eta_q\rangle$$
$$\quad \approx m^2_\pi + \frac{\sqrt{2}}{f_q}\langle 0|\frac{\alpha_s}{4\pi}G\tilde{G}|\eta_q\rangle,$$
$$m^2_{\eta_s} = \frac{2}{f_s}\langle 0|m_s\bar{s}i\gamma_5 s|\eta_s\rangle + \frac{1}{f_s}\langle 0|\frac{\alpha_s}{4\pi}G\tilde{G}|\eta_s\rangle$$
$$\quad \approx 2m^2_K - m^2_\pi + \frac{1}{f_s}\langle 0|\frac{\alpha_s}{4\pi}G\tilde{G}|\eta_s\rangle, \tag{A10}$$

where contributions to their masses from the gluonic anomaly have been included. We shall use the parameters extracted from a phenomenological fit [3]:

$$\frac{1}{\sqrt{2}f_q}\langle 0|\frac{\alpha_s}{4\pi}G\tilde{G}|\eta_q\rangle = 0.265 \pm 0.010,$$
$$\frac{\langle 0|\frac{\alpha_s}{4\pi}G\tilde{G}|\eta_q\rangle}{\sqrt{2}\langle 0|\frac{\alpha_s}{4\pi}G\tilde{G}|\eta_s\rangle} = \frac{f_s}{f_q}. \tag{A11}$$

Numerically,

$$h^q_\eta = 0.0013 \text{ GeV}^3, \qquad h^s_\eta = -0.0555 \text{ GeV}^3,$$
$$h^q_{\eta'} = 0.0011 \text{ GeV}^3, \qquad h^s_{\eta'} = 0.068 \text{ GeV}^3,$$
$$f^q_\eta = 109 \text{ MeV}, \qquad f^s_\eta = -111 \text{ MeV},$$
$$f^q_{\eta'} = 89 \text{ MeV}, \qquad f^s_{\eta'} = 136 \text{ MeV}, \tag{A12}$$
$$f^c_\eta = -2.3 \text{ MeV}, \qquad f^c_{\eta'} = -5.8 \text{ MeV},$$
$$m_{\eta_q} = 741 \text{ MeV}, \qquad m_{\eta_s} = 802 \text{ MeV},$$

where we have used the perturbative result [32]

$$f^c_{\eta^{(\prime)}} = -\frac{m^2_{\eta^{(\prime)}}}{12m^2_c}\frac{f^q_{\eta^{(\prime)}}}{\sqrt{2}}. \tag{A13}$$

[1] P. d. A. Sanchez *et al.* (*BABAR* Collaboration), Phys. Rev. D **82**, 011502 (2010).

[2] E. Barberio *et al.* (Heavy Flavor Averaging Group), arXiv:0808.1297, and online update at http://www.slac.stanford.edu/xorg/hfag.

[3] T. Feldmann, P. Kroll, and B. Stech, Phys. Rev. D **58**, 114006 (1998); Phys. Lett. B **449**, 339 (1999).

[4] H. J. Lipkin, Phys. Lett. B **254**, 247 (1991).

[5] H. Y. Cheng and C. K. Chua, Phys. Rev. D **80**, 114008 (2009).

[6] H. Y. Cheng and C. K. Chua, Phys. Rev. D **80**, 074031 (2009).

[7] M. Beneke, G. Buchalla, M. Neubert, and C. T. Sachrajda, Phys. Rev. Lett. **83**, 1914 (1999); Nucl. Phys. **B591**, 313 (2000).

[8] M. Beneke and M. Neubert, Nucl. Phys. **B675**, 333 (2003).

[9] C. K. Chua, Phys. Rev. D **78**, 076002 (2008).

[10] Z. J. Xiao, Z. Q. Zhang, X. Liu, and L. B. Guo, Phys. Rev.

D **78**, 114001 (2008).

[11] A. G. Akeroyd, C. H. Chen, and C. Q. Geng, Phys. Rev. D **75**, 054003 (2007).

[12] A. R. Williamson and J. Zupan, Phys. Rev. D **74**, 014003 (2006); **74**, 039901 (2006).

[13] W. Wang, Y. M. Wang, D. S. Yang, and C. D. Lu, Phys. Rev. D **78**, 034011 (2008).

[14] J. Schumann et al. (Belle Collaboration), Phys. Rev. D **75**, 092002 (2007).

[15] M. Bander, D. Silverman, and A. Soni, Phys. Rev. Lett. **43**, 242 (1979); S. Barshay and G. Kreyerhoff, Phys. Lett. B **578**, 330 (2004).

[16] H. Y. Cheng, C. K. Chua, and K. C. Yang, Phys. Rev. D **73**, 014017 (2006).

[17] N. Mathur et al., Phys. Rev. D **76**, 114505 (2007).

[18] S. Prelovsek, T. Draper, C. B. Lang, M. Limmer, K. F. Liu, N. Mathur, and D. Mohler, arXiv:1005.0948; S. Prelovsek and D. Mohler, Phys. Rev. D **79**, 014503 (2009).

[19] H. Y. Cheng, C. K. Chua, and C. W. Hwang, Phys. Rev. D **69**, 074025 (2004).

[20] R. H. Li, C. D. Lu, W. Wang, and X. X. Wang, Phys. Rev.

D **79**, 014013 (2009).

[21] X. Liu, Z. Q. Zhang, and Z. J. Xiao, Chin. Phys. C **34**, 157 (2010).

[22] N. Isgur, D. Scora, B. Grinstein, and M. B. Wise, Phys. Rev. D **39**, 799 (1989).

[23] D. Scora and N. Isgur, Phys. Rev. D **52**, 2783 (1995).

[24] C. S. Kim, J. P. Lee, and S. Oh, Phys. Rev. D **67**, 014002 (2003).

[25] J. H. Munoz and N. Quintero, J. Phys. G **36**, 095004 (2009).

[26] N. Sharma and R. C. Verma, arXiv:1004.1928.

[27] A. L. Kagan and A. A. Petrov, arXiv:hep-ph/9707354.

[28] A. Ali and C. Greub, Phys. Rev. D **57**, 2996 (1998).

[29] H. Y. Cheng and C. W. Chiang, Phys. Rev. D **81**, 074031 (2010).

[30] V. Mathieu and V. Vento, Phys. Lett. B **688**, 314 (2010).

[31] M. Beneke and M. Neubert, Nucl. Phys. **B651**, 225 (2003).

[32] A. Ali, J. Chay, C. Greub, and P. Ko, Phys. Lett. B **424**, 161 (1998); M. Franz, M. V. Polyakov, and K. Goeke, Phys. Rev. D **62**, 074024 (2000); M. Beneke and M. Neubert, Nucl. Phys. **B651**, 225 (2003).